Free Surface Instabilities in a Model Unbaffled Bioreactor

Irene Pieralisi[1,*], Giuseppina Montante[2], Veronica Vallini[3], Alessandro Paglianti[1]

[1]Department of Civil, Chemical, Environmental and Material Engineering, University of Bologna, via Terracini 28, 40131 Bologna, Italy
[2]Department of Industrial Chemistry "Toso Montanari", via Terracini 28, 40131 Bologna, Italy
[3]EridaniaSadam, via della Barchetta, 1, 60035, Jesi Ancona, Italy

*corresponding author: irene.pieralisi2@unibo.it

AbstractThe aim of this study is to investigate the fluid dynamics behavior of a stirred tank resembling at lab scale the typical design of a bioreactor adopted industrially for the production of biogas by fermentation of agricultural scraps. The system consists of a partially filled, flat bottomed, unbaffled cylindrical vessel, stirred by dual A310 impeller.
The ensemble-averaged velocity fieldsare determined by Particle Image Velocimetry (PIV), in selected portions of a diametrical vertical plane of the vessel, in order to account for the strong variations of the flow moving from the impeller region towards the vessel wall. The system is studied for rotational Reynolds numbers ranging from 32000 up to 96000.
Due to the unconventional geometry of the mixing apparatus, peculiar interactions arise among the strong tangential motion of the flow, the impeller discharge stream and the flow free surface, producing relevant changes in the flow pattern and making the measurement of the flow field particularly challenging.
Thevariations of the flow are proved to be directly related to the oscillation of the liquid free surface.This relationship is further confirmed studying the characteristic frequencies of the flow, which are derived from frequency analysis of the velocity time series collected with both PIV and a Pitot system
Having assessed the extensive influence exerted by the motion of the gas-liquid interface on the overall system fluid dynamics, and considering its huge potential impact on mixing performances, a deep characterization of the phenomenon is carried out.

Keywords: Unbaffled stirred digester, Multiple impeller, Flow instability, Particle Image Velocimetry.

1 Introduction

Mixing is a crucial unit operation in the chemical and biochemical industry, and often it is performed in mechanically stirred tanks, thanks to their ease of construction and versatility of operation.
The geometry of the mixing system can vary widely, depending on the characteristics of the process carried out: blending of miscible liquids, dispersion of gases or immiscible liquids into a liquid phase, solids suspension, chemical or biological reactions, etc.
In any case, it is well-known that the performances of the mixing equipment are strongly dependant on the three-dimensional flow generated by the stirrer, as it affects heat and mass transfer as well as the chemical reactions involved in the operation (Derksen, 2003).
Many experimental and computational investigations have been carried out in the past 50 years, and a plethora of information is available in the literature regarding the flow and mixing dynamics taking place in a stirred tank of *standard geometry* (baffled vessels with $H/T \geq 1$, and $1/3 \leq D/T \leq 1/2$).
However, in industrial applications, reactors of unconventional configuration are often employed, a particular case being that of industrial digesters for the wet fermentation of organic scraps, which are unbaffled tanks stirred with single or multiple coaxial impellers of small diameter to tank diameter ratio and partial fluid fillings.
The available knowledge gained so far on the fluid and mixing dynamics encountered in reactors of such type is quite narrow (e.g. Motamedvaziri and Armenante, 2012; Montante and Paglianti, 2015), and general predictive equations cannot be applied to calculate power consumption, flow number and mixing time, as these parameters are strictly related to the different hydrodynamics produced by the impellers–tank interactions.
Therefore, further efforts are demanded to widen the range of geometrical configurations studied, with the aim of improving design rules and operating conditions for industrial apparatuses.

A particular category of stirred reactors, which has been investigated at a lesser extent, is represented by unbaffled tanks. Typically, in these tanks a prevailing tangential flow develops, and, depending on impeller speed and liquid height, a definite vortex may expand from the free surface, whose depth has to be carefully monitored in order to avoid impeller flooding and gas entrainment. On the contrary, in vessels equipped with baffles (typically 4 baffles at 90° from each other), the vortex formation is inhibited and the circulation of the fluid along tangential patterns is weaker. This leads to a stronger axial flow which improves the pumping flow rate and the mixing efficiency, thus making these apparatuses more suitable for many industrial applications.
Nevertheless, in some cases the use of unbaffled tanks has been shown to be convenient, as for example in food and pharmaceutical industries, where vessel cleanness is a fundamental requirement of the processes (Assirelli et al., 2008), and in biological applications where cell damage has to be avoided (Aloi and Cherry, 1996; Scargiali et al., 2012b). In solid suspension treatments, unbaffled tanks were found to give rise to higher fluid-particle mass transfer rates for a given power consumption (Grisafi et al., 1994; Yoshida et al., 2008), and to ensure complete suspension attainment with lower mechanical power, if compared to baffled vessels requirements (Brucato et al., 2010; Wang et al., 2012).
When the process involves a very viscous fluid or a two-phase mixture at high solid concentration, baffles can actually worsen the mixer performances, as they give rise to dead zones where the fluid and the solid particles tend to accumulate (Nagata, 1975; Lamberto et al., 1996; Rousseaux et al., 2001).
The use of unbaffled tanks may also be appropriate in gas-liquid processes, as oxygen mass transfer is considerably increased when agitation goes beyond the critical rotational speed, N_{cr}, and the free surface vortex reaches the impeller, with consequent bursting of bubbles inside the reactor.
For the same reason, unbaffled tanks can be adopted as self-ingesting reactors in three-phase mixing operations, allowing adequate gas transfer inside the reactor without the use of a sparger, that can be easily blocked by solid particles (Conway et al., 2002; Scargiali et al. 2014). This solution is applied in numerous biotechnological processes, for example in the case of cell cultures growth employing microcarriers spheres.
Notwithstanding unbaffled stirred reactors may be suitable for a wide range of mixing applications, a characterization of the local flow field generated inside these apparatuses has rarely been performed (Armenante et al., 1997; Alcamo et al., 2005), and so far, important hydrodynamic parameters, such as power consumption and mixing time, have been determined only for few geometrical configurations and operational conditions (Scargiali et al. 2014; Busciglio et al, 2014).
Armenante et al (1997) investigated the flow field generated by a PBT impeller in unbaffled reactors, by means of both LDA experiments and fluid dynamics computational techniques. They reported tangential velocities significantly bigger with respect to the other two components, and in vertical planes they identified a strong radial flow, forming two main recirculation loops, one above and the other below the impeller. Similar flow features were detected also by Derksen (2006) in A310 stirred reactors.
These results suggest that in unbaffled configurations, axial impellers tend to lose most of their typical pumping action, and that the majority of the kinetic energy of the fluid is consumed along the tangential direction.

In the present work, an unbaffled tank of unconventional geometry stirred with dual A310 impeller is considered ($H=T/2$, $D=T/5$).
The apparatus was obtained from the scale-down of an industrial digester, and its main hydrodynamics features have been already investigated by Montante and Paglianti (2015). In particular, power consumption and mixing time together with velocity vector fields under selected combinations of operating conditions were determined. Big differences were found comparing the mean flow field with that generated by A310 impellers in conventional geometries, and wide oscillations of the free surface were detected, highlighting the requirement of further, more detailed characterization of both the local flow field and the characteristic frequencies of the flow.
In this study, the mean velocity field and the turbulent flow characteristics are determined by Particle Image Velocimetry (PIV) in limited portions of the vessel, thus improving the accuracy of the measurements and the resolution of the velocity vector fields, as required by the strong flow inhomogeneity over the vessel volume. Moreover, the PIV velocity time traces collected in specific locations, and the pressure time traces recorded by a Pitot system are analysed by FFT, in order to identify a connection between the free surface behaviour and variations in the circulation flow pattern.
So far, the free surface flow generated in unbaffled reactors has been subjected to numerous experimental

and computational investigations, aimed at determining its main features (vortex depth and extension, etc.) and its impact on the process performances (Lamarque et al., 2010; Busciglio et al., 2013).
Notwithstanding the amount of information available on this topic, no mention has been found in the literature regarding the influence exerted on the flow field by the motion of the gas-liquid interface.
The outcomes of this work lead to identify a new type of flow macroinstability, which influences greatly the dynamics of the system, and therefore may have a relevant impact on the performances of industrial apparatuses of similar geometry.

2 Materials and Methods

The investigated stirred tank, shown in Fig. 1 consists of a partially filled, flat bottomed, unbaffled cylindrical vessel of diameter, T, equal to 0.49 m and height, H, equal to 0.255 m ($H \approx T/2$). The mechanical agitation was provided by two identical Lightnin A310 impellers of diameter, D, equal to 0.2 T, the lower of which was placed at an off-bottom clearance, C_1, equal to 0.08 T and at distance from the upper impeller, C_2, equal to 0.18 T. The impellers were mounted on a shaft coaxially with respect to the vessel axis, and demineralised water was used as the working fluid.
The reactor was studied at three different liquid heights: h_L = 0.69 H - 0.8 H - 0.92 H (17.5 cm - 20.5 cm - 23.5 cm), and for rotational Reynolds number, Re, ranging from 32000 up to 96000 (200 rpm <N< 600 rpm), therefore the flow regime was fully turbulent in all the cases investigated, at least in the vicinity of the impellers.
The ensemble-averaged velocity fields were determined by a standard PIV system, applied to selected portions of a diametrical vertical plane of the vessel, in order to account for the strong variations of the flow moving from the impeller region towards the vessel wall. A sketch of the two measurement areas analysed, is shown in Fig. 1.

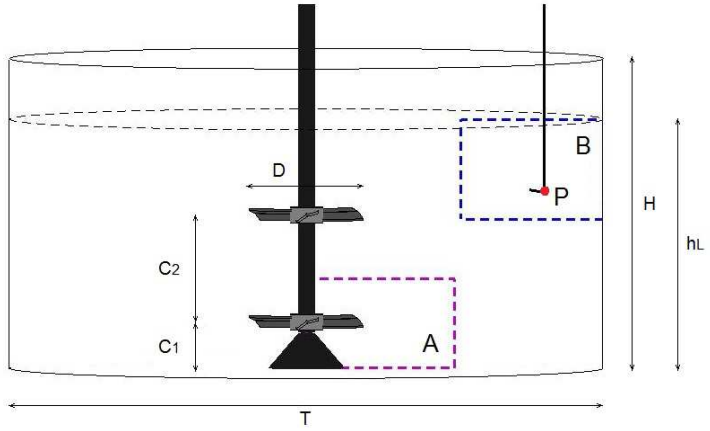

T	0.49 m
H	0.255 m
h_L	0.175 – 0.205 – 0.235 m
D	0.098 m
C_1	0.039 m
C_2	0.088 m
'zone A'	*impeller area*
'zone B'	*free surface area*
P (r/T, Θ, z/T)	(0.44, 0°,0.43-0.3)

Fig.1 Sketch of the model stirred vessel studied and measurement plane location.

The working fluid was seeded by polymeric particles coated with fluorescent Rhodamine B emitting light at the wavelength of λ = 590 nm. To minimise refraction effects at the curved surface, the vessel was placed inside a square trough filled with the working liquid. The experimental system included a LitronNd:YAG laser, emitting light at 532 nm with a maximum frequency of 15 Hz and energy equal to 65mJ, and a HiSense MK II 1344×1024 pixels CCD camera, provided with an optical filter cutting off the light wavelength lower than that emitted by the fluorescent seeding particles.
When 'zone A' was investigated, the time interval between two laser pulses was experimentally set at Δt = 850 μs for the condition N = 300 rpm, and this value was then adjusted for all the other rotational speeds considered. Close to the vessel wall ('zone B'), minor variation of the flow and lower velocity magnitudes were detected, therefore a constant value of Δt = 4000 μs was chosen at any impeller speed investigated.
PIV analysis was carried out through the use of an adaptive-correlation algorithm, applied on interrogation areas (IA) of initial size 64 x 64 pixel ('zone A'), and 128 x 128 pixel ('zone B'). Two refinement steps together with 50% overlap resulted in final windows of respectively 8 x 8 pixels and 16 x 16 pixel, allowing the reconstruction of the flow field with a spatial resolution of 2 mm in 'zone A', and of 3.7 mm in 'zone B'.
The instantaneous vectors underwent validation algorithms based on the evaluation of the peak heights in the

correlation plane, and the measurements region was then limited to the zone where at least 90% of the vectors passed the validation step.
The statistical convergence of data was checked on both mean velocities and turbulence levels, and the number of image pairs necessary to obtain reliable results was set to 1000 for each PIV experiment.
The characteristic frequencies of the flow were studied through frequency analysis of the velocity time series collected with the PIV.
To further confirm the results, a Pitot system was employed, which allowed to work with higher rates of acquisition, thus improving the resolution and the range of spectra detected.
The transducer was inserted in the reactor by a lid-port placed over the diametrical plane investigated by PIV. The pressure time series were measured in a point 'P' located at radius, $r/T = 0.44$, $\Theta = 0°$, and axial distance from the vessel bottom, $z/T = 0.43 - 0.3$, depending on the value of liquid height (see Fig. 1). After checking the influence of both acquisition rate and sampling time, a time-span ranging from 15 to 60 minutes and a sampling frequency of 500 - 800 Hz were adopted in the experiments.
The origin of the cylindrical reference system was located at the centre of the vessel bottom; all dimensions and coordinates were normalized with the tank diameter T (r/T, z/T); all mean velocities and turbulence levels were normalized with the tip blade velocity $V_{tip} = \pi ND$. The mean axial velocity, V_z/V_{tip}, was positive if directed upwards and the mean radial velocity, V_r/V_{tip}, was positive if directed towards the vessel wall.

3.Results and discussion

A preliminary visual observation of the model bioreactor allowed understanding some important features of its way of operation.
After any change in the impeller speed, a very long transient flow was detected before achieving steady state condition, as firstly reported by Montante and Paglianti (2015), and this time lapse was found dependant on both rotational speed and liquid height.
Typically, tens of seconds from the agitation onset are required in stirred tanks of "standard geometry" to attain a stable flow (e.g. Brown et al., 2004; Montante et al., 2001), while mixing systems of unconventional geometry can exhibit longer transient regimes (Pinelli et al., 2001; Derksen, 2006).
In the model bioreactor under study, significant variations of the overall flow motion were observed for approximately 45 minutes after any change in the agitation power, and this made the application of the PIV technique particularly challenging and time-consuming.
In addition, at steady-state condition peculiar free surface oscillations were observed.
At each value of h_L tested, the gas-liquid interface manifested two distinct wavelet modes, depending on the rotational speed chosen. The free surface presented either the typical outline of unbaffled stirred tanks, with a definite whirlpool vortex developing around the shaft and driving the fluid tangentially towards the vessel wall (Busciglio et al., 2013), or it exhibited wide 3-D oscillations, with a frequency well below that of the blades passage and a superficial vortex rotating eccentrically around the shaft. A snapshot of the free surface motion in this last case is shown in Fig. 2.

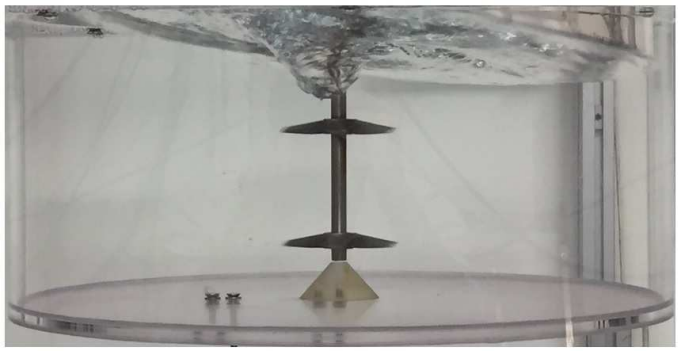

Fig. 2 Snapshot of the stirred tank working with $h_L = 0.205$ m, at$N = 300$ rpm ($Re = 48020$).

PIV technique was used to assess the mean flow patterns generated by the A310 impellers in steady-state conditions in selected portions of a diametrical vertical plane of the vessel.
Fig. 3 shows the velocity vector fields superimposed to the contour maps of the tangential component of the vorticity, $\omega_\theta/(\pi N)$, averaged over 1000 instantaneous measurements in the impeller region, obtained at a liquid height h_L = 0.235 m and varying the Reynolds number.

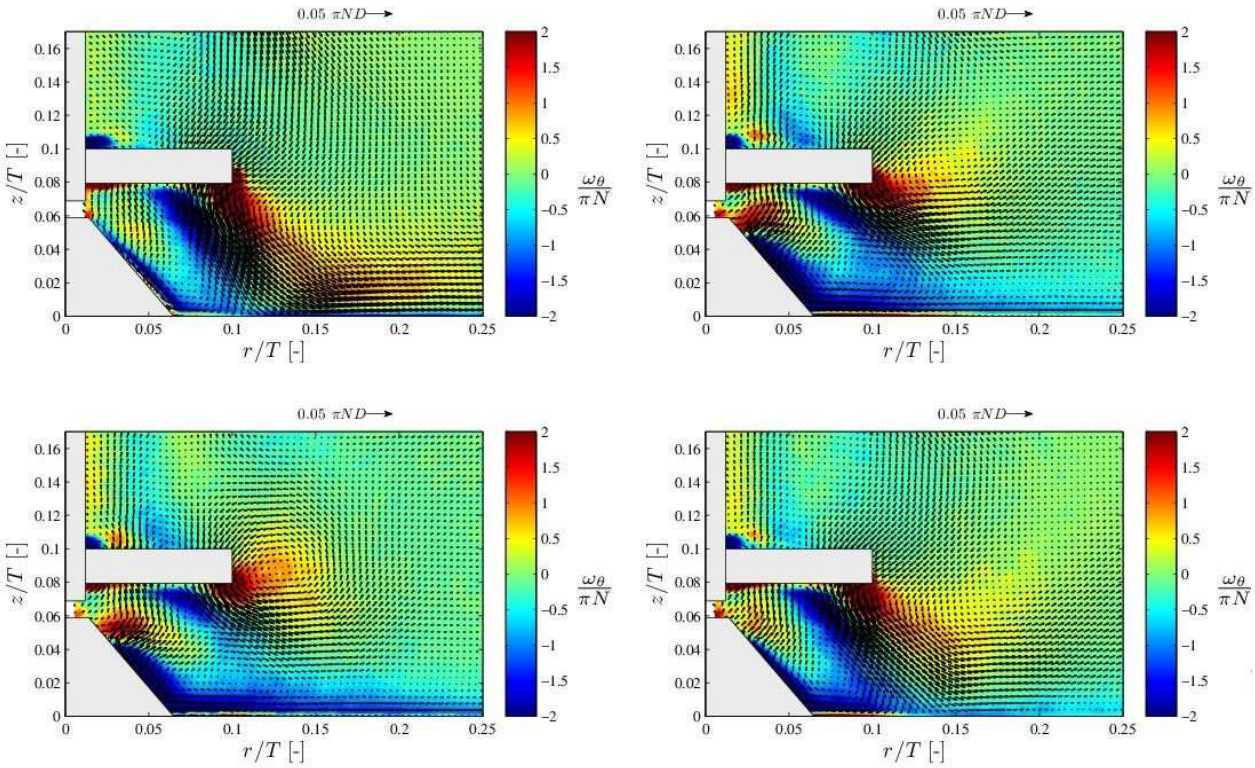

Fig. 3 Ensemble-averaged flow field and contour map of the tangential component of the vorticity, $\omega_\theta/(\pi N)$, in the impeller region (*zone 'A'*). h_L = 0.235 m , (a) N = 250 rpm (Re = 40017); (b) N = 330 rpm (Re = 52822) ; (c) N = 400 rpm (Re = 64027) ; (d) N = 230 rpm (Re = 36815).

At N = 250 rpm (Re = 40017), the impeller discharge stream is strongly axial, with mean velocities exhibiting an average inclination of 65° from the horizontal direction (Fig. 3-a). Under the thrust of the turbine, the fluid reaches the bottom of the tank and attaches to it flowing towards the wall, while for r/T< 0.1, a definite recirculation zone appears below the impeller.
As N increases (Fig. 3-b), the turbine jet starts to tilt radially, and at N = 400 rpm (Re = 64027), it is completely lifted from the bottom (Fig. 3-c).
Observing the specific flow features close to vessel basis, an elongated area of negative vorticity appears in Fig. 3-b and 3-c, suggesting that at these stirring conditions the recirculation zone expands, and more liquid heads for the centre of the reactor, due to the orientation of the impeller discharge stream.
The flow field measured at N = 250 rpm (Fig 3-a) is closer to that typically obtained in standard baffled tanks stirred with A310 impellers (e.g. Bugay et al., 2002), since in both cases the impeller loop reaches the bottom of the vessel and runs towards the lateral wall, while after the occurrence of the flow transition (Fig 3-b-c), the main circulation loop changes completely its features.
Flow patterns similar to the one depicted in Fig 3-c were detected increasing the rotational speed, while reducing backwards the value of N, the system tended to return to its initial configuration. This is the case shown in Fig. 3-d for N = 230 rpm (Re = 36815).
An analogous switch of the flow pattern between two stable configurations was detected inside the reactor for liquid heights h_L = 0.175 m and h_L =0.205 m, at different values of Reynolds number.
The evolution of the impeller discharge stream from primarily axial to radial was further confirmed analysing the magnitude and distribution of kinetic energy in the impeller region, where k'_{rz} was derived

from 2-D turbulent velocity data and assuming isotropy for the unknown tangential component (Gabriele et al., 2011):

$$k'_{rz} = \frac{2}{3}(u'^2_r + u'^2_z) \qquad \text{(Eq. 1)}$$

Fig. 4 shows the contour maps of $k'_{rz}/(\pi ND)^2$, at h_L = 0.235 m. In the first image (Fig 4-a), representing the system at N = 250 rpm, the impeller discharge stream is highlighted by a zone with high energy content developing axially below the impeller. After the onset of the flow transition, the kinetic energy distribution evolves, with a radially tilted jet appearing at N = 400 rpm (Fig. 4-b).

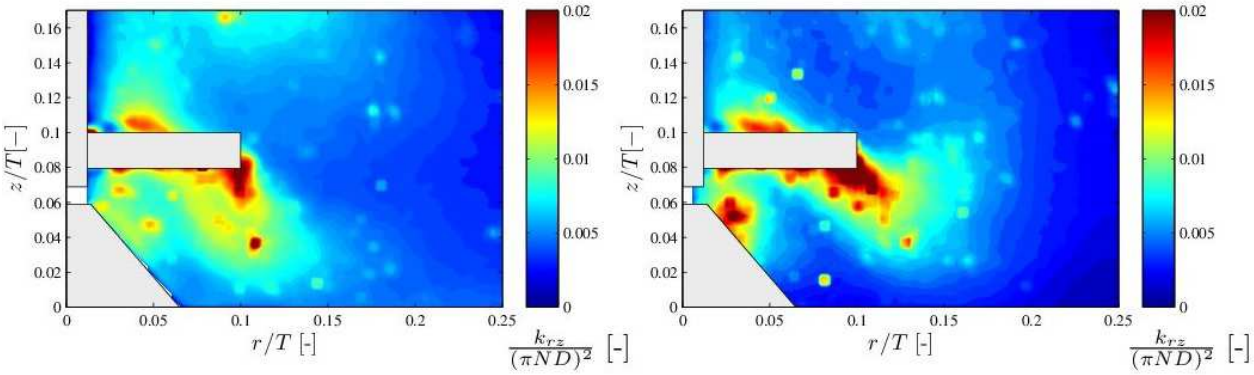

Fig. 4 Contour map of the turbulent kinetic energy, $k_{rz}/(\pi ND)^2$, in the impeller region (*zone 'A'*). h_L = 0.235 m , (a) N = 250 rpm (*Re* = 40017); (b) N = 330 rpm (*Re* = 52822).

In any case, the results outline that the turbulent content of the flow varies widely depending on the radial location considered, and this may have important consequences if turbulence affected processes, such as solid suspensions and draw down, are carried out inside the tank.
In particular, in Fig. 4-b the turbulent motion of the fluid appears confined to the impeller region, while for radial locations r/T> 0.17 the turbulent fluctuations decrease very sharply.
Considering this, it may be argued that the suspension of a solid substrate in the present geometrical configuration would be hardly achievable, even at higher impeller speeds (Montante and Paglianti, 2015).

PIV experiments were carried out in the upper corner of the tank ('*zone B*'), to assess the effect of the flow transition in locations far away from the impeller.
Fig. 5 shows ensemble-averaged velocity vector fields and contour maps of the tangential component of the vorticity, $\omega_\theta/(\pi N)$, obtained at h_L = 0.235 m. The images disclose net differences between the two velocity patterns.The flow field generated at N = 200 rpm (Fig. 5-a) is characterized by a circulation across the whole area investigated, where the fluid climbs up the lateral vessel wall, and then is recalled towards the centre of the tank by the pumping action of the turbines.
On the contrary, at N = 400 rpm (Fig. 5-b) the flow pattern is less definite, and the velocities have lower magnitude, suggesting again that after the flow transition, the circulation of the fluid in regions located far away from the impeller is very limited.
It is worth observing that the wide free surface oscillations occurring at this agitation speed are expected to greatly affect the instantaneous vector fields measured in the vicinity of the gas-liquid interface, therefore, the ensemble averaged velocity field may not be adequate to properly depict the intrinsically transient behaviour of the flow.

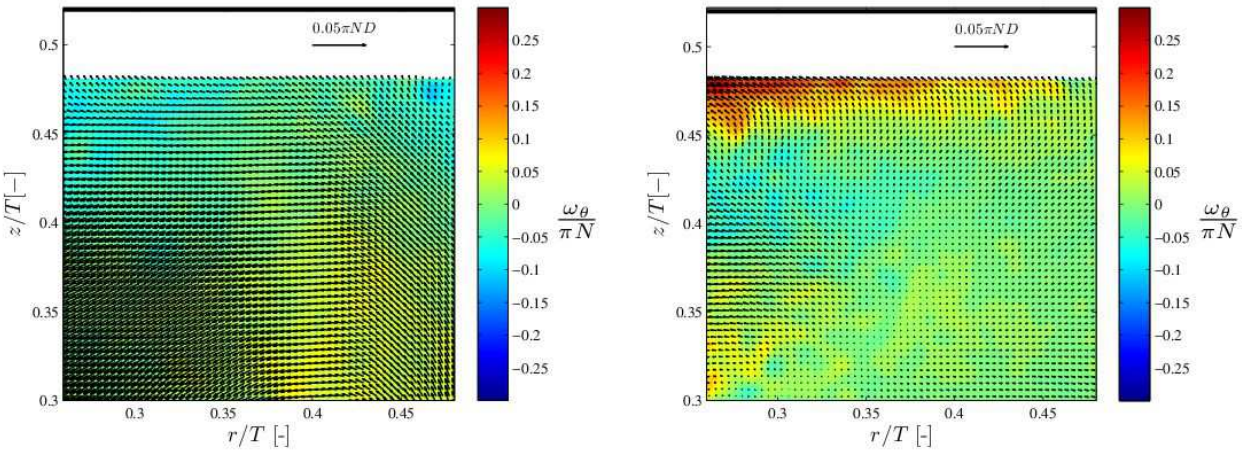

Fig. 5 Ensemble-averaged flow field and contour map of the tangential component of the vorticity, $\omega_\theta/(\pi N)$, close to the system free surface and to the vessel wall (*zone 'B'*). h_L = 0.235 m , (a) N = 200 rpm (Re = 32013) ; (b) N = 400 rpm (Re = 64027).

All the results outlined so far, denote the presence of a flow transition, manifesting itself as the switching between two different stable flow patterns, one taking place at lower *Re*, and another at higher *Re*number, depending on the value of liquid height set inside the reactor.
Matching preliminary free surface observations with PIV results, the transition was proved to be directly related to the behaviour of the system free surface, as a sharp correspondence between the flow field variations and the wavelet mode exhibited by the gas-liquid interface was found at any value of h_L tested.
In particular, it can be concluded that the onset of wide free surface oscillations inside the reactor, occurring at specific values of impeller speed, triggered the flow transition, and thus was the origin of the changes detected in the velocity patterns.
Having assessed the extensive influence exerted by the free surface motion on the overall system fluid dynamics, and considering its huge potential impact on mixing performances, a deep characterization of the phenomenon was deemed crucial.

From PIV data obtained in the impeller region ('zone A'), the inclination of the turbine discharge flow with respect to the horizontal axis, Θ, was analysed varying the agitation power.
Starting from the condition of still fluid (N = 0), the impeller rotational speed was increased by successive steps of 50 rpmup to N = 600 rpm, and after the attainment of steady-state condition, information regarding Θ were collected. Subsequently, the same procedure was applied reducing backwards the value of N.
Fig. 6 shows the result of this analysis for the condition h_L = 0.235 m. Looking at the graph, the angle Θ assumes an almost constant value of 65° for low values of the agitation speed ('*segment 1'*), however at N = 330 rpm, the curve exhibits a sudden drop, and the inclination of the impeller jet turns to 25° ('*segment 2'*).
This reveals a deflection of the turbine pumping action towards the radial direction, and corresponds to the onset of the peculiar free surface oscillations previously described (Fig. 2-b).
No significant variations of Θ were detected increasing further the rotational speed ('*segment 3'*), while reducing it backwards, for $N \leq 250$ rpm, the inclination of the impeller discharge flow assumed again a value of ≈ 65° ('*segment 4'*), meaning that the velocity pattern and the free surface returned to their initial configurations.
Yet, a scrutiny of Fig. 6 highlights that there is a delay of ΔN_{delay} = (330-250) rpm = 80 rpm, between '*segment 2'* and '*segment 4'*, suggesting that the flow transition exhibits an hysteresis, and that once the phenomenon has been triggered, it tends to endure, even when the agitation power goes below the value needed to prompt it.

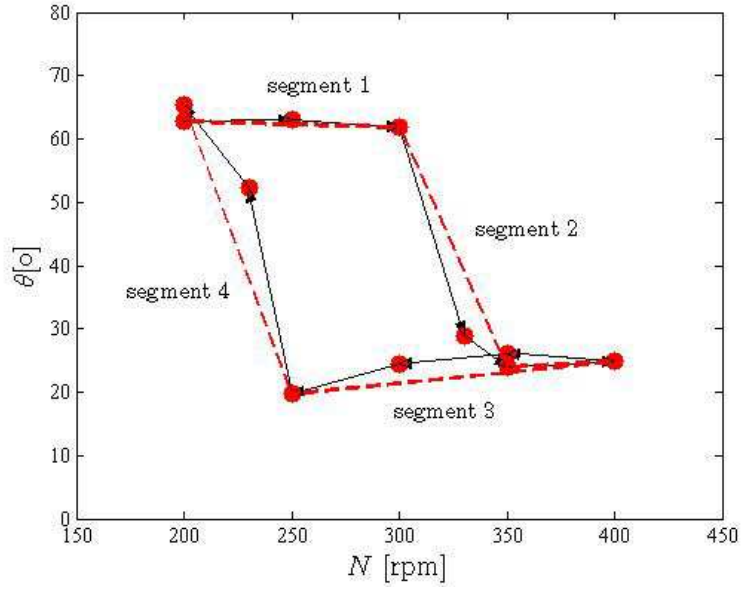

Fig. 6 Variation of the impeller angle discharge stream, Θ, with the rotational speed, N at h_L = 0.235 m .

The relationship found between the visually observed gas-liquid interface motion and the mean flow field is further confirmed by a quantitative evaluation of the characteristic frequencies of the flow, which were derived from the frequency analysis of the velocity time series collected with the PIV, and the Pitot system.
The efficacy of the latter technique has already been established in previous investigations for the detection of macroinstabilities in stirred reactors (Paglianti et al, 2006), and in the present study it was used to validate the results obtained from the frequency analysis of the PIV time series, due to much higher acquisition rates (ranging from 500 to 800 Hz) and total number of instantaneous data collected (up to 1 million points).
Both systems yielded analogous results, but for brevity of presentation, only those obtained with the Pitot system are presented below.
The signal time traces shown in Fig. 7 were measured in the location 'P' of the tank shown in Fig. 1 (r/T = 0.44; Θ = 0°; z/T= 0.43), for a liquid height h_L = 0.235 m, and at rotational speeds of N = 300 rpm (Figure 7-a), and N = 350 rpm (Figure 7-b), respectively. In the images, the time scale is limited to a maximum of 5 s for a clearer visualization.

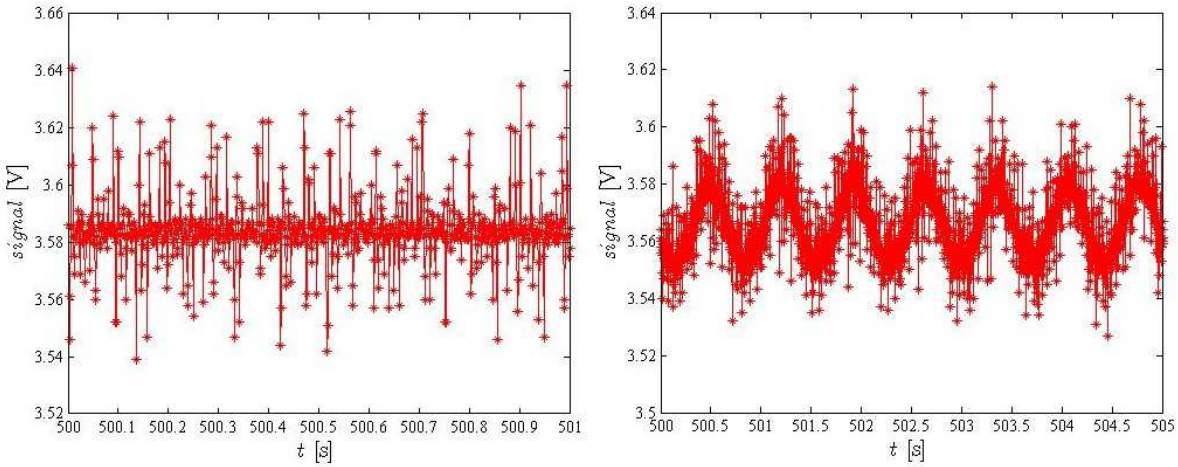

Fig. 7 Time serie of the voltage signal obtained with Pitot system in the location 'P' (r/T = 0.44, Θ = 0°, z/T = 0.43), at h_L = 0.235 m. (a) N = 300 rpm (Re = 48020), acquisition frequency, f_{ac} = 800 Hz ; (a) N = 350 rpm (Re = 56023), acquisition frequency, f_{ac} = 500 Hz.

Before the occurrence of the flow transition, the voltage signal exhibits significant fluctuations, but a dominant frequency cannot be identified (Fig. 7-a).
On the contrary, looking at Fig. 7-b the signal manifests a definite cyclic variation, whose characteristic period is approximately equal to 0.7 s, corresponding to a frequency, f , equal to 1.4 Hz.

A FFT analysis implemented in the MatLab software was used to obtain spectral distributions of the dynamic voltage signal, and the results confirmed the observations made on the time series.
In Fig. 8-a the frequency spectrum obtained at N = 300 rpm, thus before the appearance of the wide free surface oscillations and the modification of the impeller discharge stream from strongly axial to mainly radial, is shown. Many peaks of very little amplitude appear (order of magnitude 10^{-3}), but none of them is deemed prevailing. The shaft frequency (5 Hz) does not show a marked impact on the spectrum, and this can be explained considering that the measurement point was located far away from the impeller, at r/D = 2.2.
Different results were obtained when the rotational speed was set to a value that ensured the flow transition. This is the case depicted in Fig. 8-b, where N = 350 rpm.

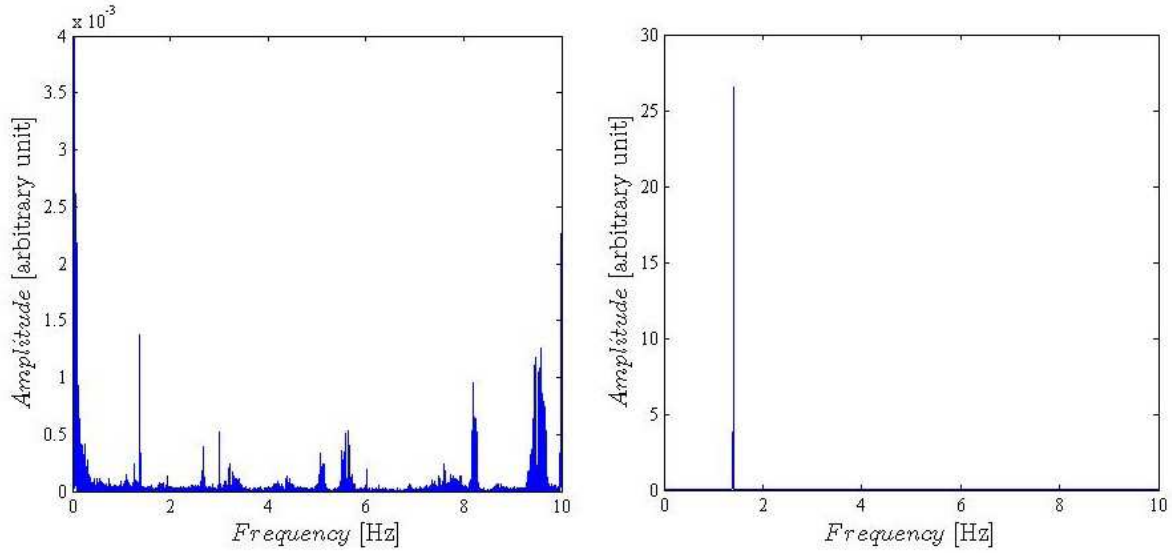

Fig. 8 Frequency spectrum of the voltage signal obtained with Pitot system in the location 'P' (r/T = 0.44, Θ = 0°, z/T = 0.43), at h_L = 0.235 m. (a) N = 300 rpm (Re = 48020), acquisition frequency, f_{ac} = 800 Hz ; (a) N = 350 rpm (Re = 56023), acquisition frequency, f_{ac} = 500 Hz.

As can be observed, the spectrum exhibits a very pronounced and narrow peak at f = 1.4 Hz, suggesting that a well-defined periodic phenomenon manifests in the flow with this characteristic frequency.
This dominant event was identified in the wide oscillations of the gas-liquid interface occurring approximately every 1 second at N = 350 rpm.
The results just outlined, prove the existence of a peculiar macro-instability of the flow, generated for selected operational conditions by the behaviour of the system free surface, and responsible of the flow transition detected by the velocity field measurements.

The spectral analysis was repeated on a wider range of conditions, to investigate the influence of the agitation power on the macroinstability frequency. The system was studied at different values of liquid height, in a range of rotational speeds ensuring the oscillatory motion of the gas-liquid interface.
Observing the results shown in Fig. 9, it can be noticed that the data collected at different impeller speeds display all a weak increase of the frequency for increasing values of h_L. Also, increasing the agitation speed, only a very slight increment of $f$occurs, for any value of h_L set inside the tank.
This finding proves that the flow instability detected differs from any of those identified in the past, as a definite linear dependency of the frequency on the rotational speed has been typically reported in the available literature on macro-instabilities (e.g. Nikiforaki et al., 2003; Paglianti et al., 2006).

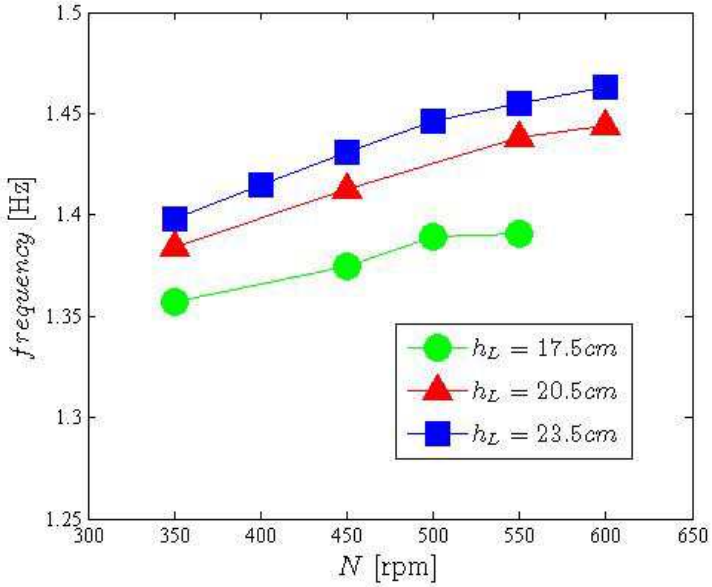

Fig. 9 Influence of the rotational speed, N, on the macroinstability frequency, f. System studied at different liquid heights, h_L.

4. Conclusions

The fluid dynamic analysis of the lab-scale model digester, based on the collection of detailed velocity measurements and on the identification of the characteristic frequencies of the motion, has revealed the relationship between the frequency of the liquid free surface oscillations and the liquid flow field, which experiences a significant modification depending on the impeller speed and the filling height. The transition of the flow field between two very different stable configurations is associated to the variations of the impeller discharge flow inclinations, that moves from typically axial to radial. The results of the present investigation highlight a flow instability never detected so far, which is probably associated to the specific geometrical characteristics of the investigated stirred tank.
These findings are of great relevance for the correct operation of the industrial digesters adopted for the wet fermentation of organic substrates, whose proportions among the main geometrical dimensions (impeller diameter to tank diameter ratio, filling height) are often very close to those of the investigated stirred tank.
Future work will be devoted to identify a possible quantitative correlation among the geometrical and operational parameters, in order to be able to predict and avoid the onset of the flow instabilities, which are expected to cause severe problems to the operation of the industrial apparatuses.

References

[1] Derksen J J (2003) Numerical simulation of solids suspension in a stirred tank. *AIChE Journal*, vol. 49, pp 2700-2714.

[2] Motamedvaziri S and Armenante P M (2012) Flow regimes and surface air entrainment in partially filled stirred vessels for different fill ratios. *Chemical Engineering Science*, vol. 81, pp 231–250.

[3] Montante G and Paglianti A (2015) Fluid dynamics characterization of a stirred model bio-methanation digester. *Chemical Engineering Research and Design*, vol. 93, pp 38-47.

[4] Assirelli M, Bujalski W, Eaglesham A, Nienow A W (2008) Macro- and micromixing studies in an unbaffled vessel agitated by a Rushton turbine. *Chemical Engineering Science*, vol. 63, pp 35–46.

[5] Aloi L E and Cherry R S (1996) Cellular response to agitation characterized by energy dissipation at the impeller tip. *Chemical Engineering Science,* vol. 51 (9), pp 1523–1529.

[6] Scargiali F, Busciglio A, Grisafi F, Brucato A (2012b) Oxygen transfer performance of unbaffled stirred

vessels in view of their use as biochemical reactors for animal cell growth. *Chemical Engineering Transactions,* vol. 27, pp 205–210.

[7] Grisafi F, Brucato A, Rizzuti L (1994) Solid–liquid mass transfer coefficient in mixing tanks: influence of side wall roughness. *IChemE Symposium Series*, n 136, pp 571–578.

[8] Yoshida M, Kimura A, Yamagiwa K, Ohkawa A, Tezura S (2008) Movement of solid particles on and off bottom of an unbaffled vessel agitated by unsteadily forward–reverse rotating impeller. *Journal of Fluid Science and Technology,* vol. 3 (2), pp 282–291.

[9] Brucato A, Cipollina A, Grisafi F, Scargiali F, Tamburini A (2010) Particle suspension in top-covered unbaffled tanks. *Chemical Engineering Science*, vol. 65, pp 3001–3008.

[10] Wang S, Boger D V, Wu J (2012) Energy efficient solids suspension in an agitated vessel-water slurry. *Chemical Engineering Science,* vol. 74, pp 233–243.

[11] Nagata S (1975) Mixing Principles and Applications. Halsted Press, New York.

[12] Lamberto D J, Muzzio F J, Swanson P D, Tonkovich A L (1996) Using time dependent RPM to enhance mixing in stirred vessels. *Chemical Engineering Science*, vol. 51, pp 733–741.

[13] Rousseaux J M, Muhr H, Plasari E (2001) Mixing and micromixing times in the forced vortex region of unbaffled mixing devices. *Canadian Journal of Chemical Engineering,* vol. 79, pp 697–707.

[14] Conway K, Kyle A, Rielly C (2002) Gas–liquid–solid operation of a vortex-ingesting stirred tank reactor. *Chemical Engineering Research and Design,* Part A, vol. 80, pp 839–845.

[15] Scargiali F, Busciglio A, Grisafi F, Brucato A (2014) Mass transfer and hydrodynamic characteristics of unbaffled stirred bio-reactors: influence of impeller design. *Biochemical Engineering Journal*, vol. 82, pp 41–47.

[16] Armenante P, Luo C, Chou C-C, Fort I, Medek J (1997) Velocity profiles in a closed, unbaffled vessel: comparison between experimental LDV data and numerical CFD predictions. *Chemical Engineering Science*, vol. 52, pp 3483-3492.

[17] Alcamo R, Micale G, Grisafi F, Brucato A, Ciofalo M (2005) Large-eddy simulation of turbulent flow in an unbaffled stirred tank driven by a Rushton turbine. *Chemical Engineering Science*, vol. 60, pp 2303–2316.

[18] Busciglio A, Grisafi F, Scargiali F, Brucato A (2014) Mixing dynamics in uncovered unbaffled stirred tanks, *Chemical Engineering Journal*, vol. 254, pp 210-219.

[19] Derksen J J (2006) Long-time solids suspension simulations by means of a large-eddy approach. *Chemical Engineering Research and Design*, vol. 84, pp 38–46.

[20] Lamarque N, Zoppe B, Lebaigue O, Doilias Y, Bertrand M, Ducros F (2010) Large-eddy simulation of the turbulent free-surface flow in an unbaffled stirred tank reactor. *Chemical Engineering Science*, vol. 65, pp 4307–4322.

[21] Busciglio A, Caputo G, Scargiali F (2013) Free-surface shape in unbaffled stirred vessels: experimental study via digital image analysis, *Chemical Engineering Science*, vol. 104, pp 868–880.

[22] Brown D A R, Jones P N, Middleton J C (2004) Experimental methods. In: Paul E L, Atiemo-Obeng V A, Kresta S M (Eds.), Handbook of Industrial Mixing: Science and Practice. Wiley-Interscience, Hoboken, NJ, pp. 183–184 (Chapter 4).

[23] Montante G, Lee K C, Brucato A, Yianneskis M (2001) Numerical simulations of the dependency of flow pattern on impeller clearance in stirred vessels. *Chemical Engineering Science*,vol. 56, pp 3751–3770.

[24] Pinelli D, Nocentini M, Magelli F (2001) Solids distribution in stirred slurry reactors: influence of some mixer configurations and limits of the applicability of a simple model for predictions. *Chemical Engineering Communications*, vol. 188, pp 91–107.

[25] Bugay S, Escudié R, Liné A (2002) Experimental analysis of hydrodynamics in axially agitated tank. *AIChE Journal*, vol. 48, pp 463–475.

[26] Gabriele A, Tsoligkas A N, Kings I N, Simmons M J H (2011) Use of PIV to measure turbulence modulation in a high throughput stirred vessel with the addition of high Stokes number particles for both up- and down-pumping configurations. *Chemical Engineering Science*, vol. 66, pp 5862–5874.

[27] Paglianti A, Montante G, Magelli F (2006) Novel experiments and a mechanistic model for macroinstabilities in stirred tanks. *AIChE Journal*, vol. 52, pp 426–437.

[28] Nikiforaki L, Montante G, Lee KC, Yianneskis M (2003) On the origin, frequency and magnitude of macro-instabilities of the flows in stirred vessels. *Chemical Engineering Science*, vol. 58, pp 2937–2949.